Modeling Structural Disorder within Single Poly(*p*-phenylenebenzobisoxazole) Fibers Using a Submicrometer Synchrotron Beam

Richard J. Davies,* Manfred Burghammer, and Christian Riekel

European Synchrotron Radiation Facility, B.P. 220, F-38043 Grenoble Cedex, France

Received September 1, 2004; Revised Manuscript Received November 23, 2004

ABSTRACT: Scanning X-ray microdiffraction has been carried out across single polymeric fibers using a beam profile of 0.1 μm across the fiber axis. As-spun and heat-treated poly(*p*-phenylenebenzobisoxazole) (PBO) fibers have been studied to investigate the influence of heat treatment on fiber structure. Meridional "layer line" scattering intensity is observed to vary across the fiber width. This can be related to variations in the degree of structural order. Through the association of disordered regions with a layered morphology, a fiber model has been developed. The model proposes a three-layer fiber morphology with gradual transitions between layers. The core region can be offset from the geometric center of the fiber, and also be asymmetric. For fitting of the model to experimental data, a Monte Carlo simulation approach is employed. For both PBO fiber types, the fiber model provides a good fit to the experimental results obtained. The modeling results indicate that the heat treatment process causes a number of morphological changes within the fiber. These include a reduction in the thickness of the fiber skin and a distortion of the fiber core. Thus, the morphological core of the heat-treated fiber does not coincide with the geometric fiber center and is highly asymmetric. Several as yet unexplained results are also reported such as a larger core size in the heat-treated fiber type.

Introduction

Fiber mechanical properties depend strongly upon fiber morphology. Studies of these relationships are often based upon an assumption of a radially isotropic single-fiber cross-section. Microscopically, many fibers exhibit radial anisotropy. This "skin−core" morphology is particularly evident in wet-spun fibers such as poly(*p*-phenyleneterephthalamide) or PPTA. Such variations are thought to influence fiber mechanical properties[1−3] and can be attributed to the fiber manufacturing process.[4,5] For example, variations in the fracture strength of single PPTA fibers have previously been attributed to a skin−core morphology.[1] Understanding the complex relationships between microscopic fiber structure and macroscopic mechanical properties may eventually provide a route to tailor specific fiber properties through the modification of skin−core morphology during processing.

Several previous studies have examined skin−core morphology in fibers such as PPTA.[2−4,6−9] Panar et al. have proposed a model consisting of well-packed and uniform fibrils in the fiber skin, with the fiber core region being more disordered.[6] While several later studies are in general agreement with this model,[3,7] they are based upon data obtained using transmission electron microscopy (TEM), scanning electron microscopy (SEM), and atomic force microscopy (AFM). Such techniques are only capable of probing localized features and require extensive sample preparation. Wide-angle X-ray scattering with a microfocused beam (μ-WAXS) provides an alternative method which is ideally suited to the study of morphological variations within single fibers. This has already been demonstrated successfully for studying across-fiber variations in a number of different fiber types.[5,10−12] This includes a recent study on PPTA which utilized waveguide optics to obtain a submicrometer beam profile.[13]

In this paper we report on the influence of heat treatment on fiber morphology. This is based on μ-WAXS of the poly(*p*-phenylenebenzobisoxazole) (PBO) fiber type using waveguide optics. A novel method of investigating (and modeling) a layered skin−core fiber structure is employed. This enables changes in morphology during the heat treatment process to be highlighted. Unlike previous studies, variations in the scattering intensity of the meridional layer lines will be used as the basis of the model. This provides a direct assessment of local organization. The technique offers important advantages over other morphological modeling approaches[13] such as the fact that crystallographic texturing and similar influences can be neglected.

Experimental Methods

Materials. Two varieties of PBO fibers are investigated in this study. Both are produced commercially by Toyobo (Japan) under the tradename Zylon. The production process involves dry-jet wet-spinning the polymer from a nematic dope through an air gap. Coagulation of the fibers occurs in an aqueous solution.[14−18] Following tension drying, production of the as-spun (AS) fiber is complete. The high-modulus (HM) variety of PBO is given a subsequent heat treatment process.[15,18] This leads to an improvement in the mechanical properties of the fiber.[15,18] The tensile moduli of the PBO AS and HM varieties are approximately 180 and 254 GPa, respectively.[19] The polymeric repeat unit of the PBO fiber is shown in Figure 1.[17]

Waveguide μ-WAXS. μ-WAXS of PBO was carried out using one-dimensional waveguide optics at the European Synchrotron Radiation Facility (ESRF) on the microfocus beamline (ID13). A short sample of fiber, approximately 4 mm in length, was glued at one end onto a glass capillary using cyanoacrylate adhesive. After curing, the capillary was mounted onto the beamline positioning stage and the free end of the fiber sample aligned to the exit of the waveguide.

* To whom correspondence should be addressed. Phone: +33 (0) 476 88 2961. Fax: +33 (0) 476 88 2904. E-mail: rdavies@esrf.fr.

10.1021/ma048209a CCC: $30.25
Published on Web 03/18/2005

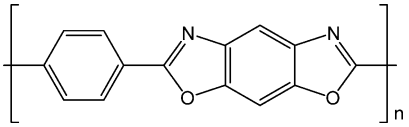

Figure 1. Polymeric repeat unit of PBO. Reprinted with permission from ref 17. Copyright 1990 VCH Publishing.

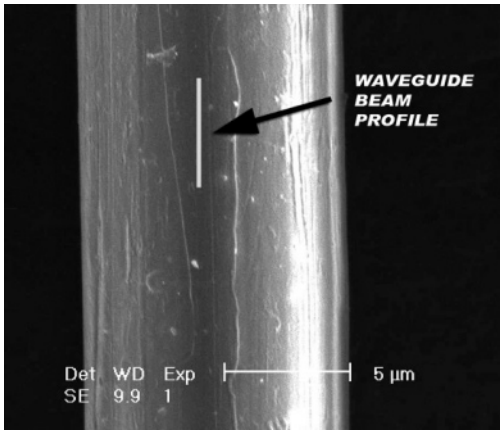

Figure 2. Schematic representation of the waveguide beam profile superimposed to scale upon an SEM micrograph of a PBO HM fiber. Note that, experimentally, both the beam and fiber are horizontal.

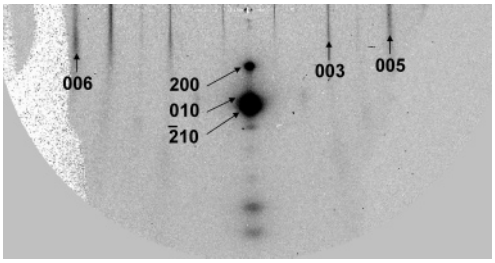

Figure 3. One hemisphere of a typical diffraction pattern generated from the center of a PBO HM fiber, indexed after Fratini et al.[23]

The X-ray waveguide provides a beam of approximately 0.1 μm in the vertical plane at its exit. The horizontal dimension of the beam is defined by the beam profile entering the waveguide and was approximately 3 μm in this instance. The experiments on PBO were performed using the TE_0 mode, which has a divergence of approximately 1 mrad.[13,20] Thus, the vertical beam size on the fiber at the exit of the waveguide cannot be larger than 0.2 μm.[13] Figure 2 shows a schematic representation of the waveguide beam profile. The profile has been superimposed proportionally onto an SEM micrograph of a PBO HM fiber. Diffraction patterns were generated across each fiber at 0.2 μm intervals. A radiation of wavelength 0.98 Å was used, with each diffraction pattern being generated with a 30 s exposure time. The diffraction patterns were collected on a MARCCD detector with an average size resolution of 64.45 × 64.45 μm^2.

The PBO diffraction data were analyzed using a combination of the Fit2D software application[21,22] and a number of custom-written automated analysis applications. These latter applications were utilized to indirectly control Fit2D, apply intensity correction factors, and perform batched function fitting and integration operations. The intensity correction factors were applied to each diffraction pattern to eliminate variations in beam brilliance and also optimize background (air-scattering) subtraction. Figure 3 shows one hemisphere of a typical diffraction pattern from the center of a PBO HM fiber obtained using the waveguide. The most intense reflections have been indexed after Fratini et al.[23] The apparent absence of a 006 layer line on the right-hand side of Figure 3 is due to obstruction by the waveguide housing. The variation

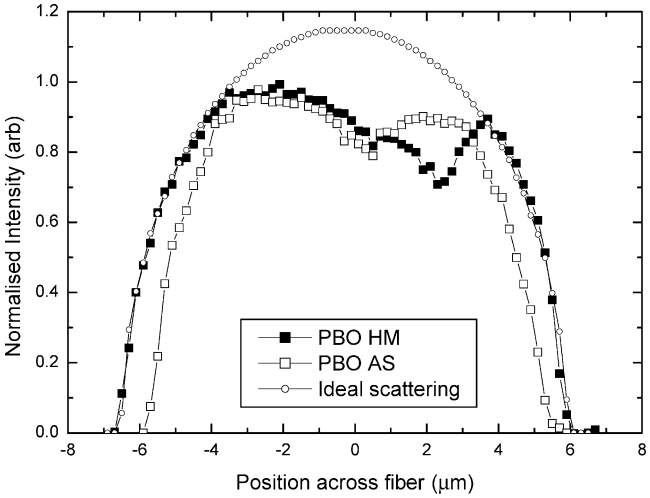

Figure 4. Across-fiber integrated intensity of the 005 layer line of single PBO AS and HM fibers, and an idealized scattering curve based upon a homogeneous, cylindrical fiber.

in meridional scattering intensity across the fiber was calculated as an average of Lorentzian fits to the integrated 005 layer lines in both hemispheres of the diffraction pattern. As only relative intensities are required, all results have been normalized to a maximum scattering intensity value of unity. It should be noted that care was taken to ensure that lateral variations in the layer line width could be excluded as an influence on the results.

Theoretical Model

Experimental Results and Model Basis. Constructive X-ray scattering corresponds to a periodicity in the electron density of the material volume irradiated by the X-ray beam. For the meridional layer lines in a fiber diffraction pattern, this periodicity relates to the axial arrangement and orientation of molecular chains. Given a homogeneous fiber, the meridional scattering intensity is proportional to the irradiated gauge volume. Any deviation from proportionality must correspond to a variation in molecular- or crystallographic-scale organization. This concept provides the basis for fiber modeling in this study. It can be clarified by considering Figure 4, which shows the meridional scattering intensities across single PBO fibers. Also plotted in Figure 4 is a calculated "ideal" scattering profile for a perfectly cylindrical and homogeneous fiber. The intensity of the ideal scattering profile has been scaled to fit the results obtained experimentally for PBO HM.

Figure 4 indicates that the across-fiber scattering profiles from both varieties of PBO do not fit to the "idealized" profile calculated for a homogeneous, cylindrical fiber. Consequently, PBO must be either heterogeneous or noncylindrical (or both). This latter possibility can be immediately excluded as SEM observations have shown PBO to exhibit a circular cross-section.[19,24,25] Thus, the intensity variations must arise due to heterogeneities. The difference between the idealized and experimental profiles can be used to approximate the amount of material irradiated by the beam not contributing to diffraction intensity. Thus, it provides an approximation of the relative degree of structural disorder within any given gauge volume.

Relating the meridional layer line scattering intensity to the degree of structural disorder requires an assumption of uniform density. However, previous studies report that the estimated ideal crystal density for PBO

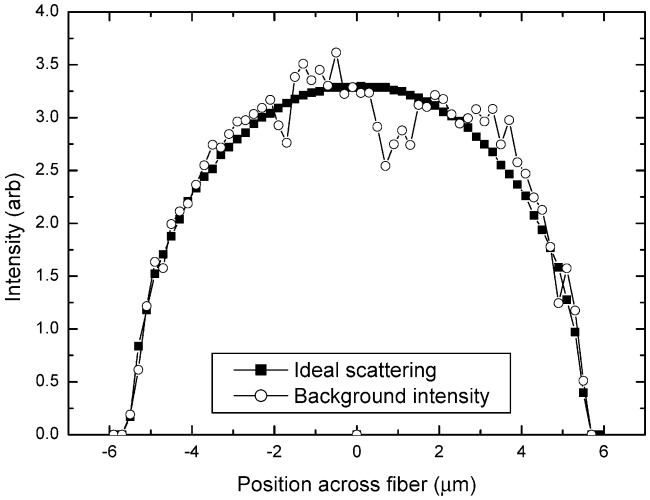

Figure 5. Across-fiber variation in the diffuse-background scattering intensity for the PBO AS fiber type and an idealized scattering curve based upon a homogeneous, cylindrical fiber.

is higher than that measured for the actual fiber.[28] In addition to this, microvoids have also been previously reported in the PBO fiber type.[14,26,27] Thus, the variations shown in Figure 4 could be attributable to a core region with a lower content or a higher void density. To assess these possibilities, the variation in diffuse-background scattering across the fiber width can be determined. This background intensity arises due to scattering from crystallites randomly arranged within the fiber. Figure 5 shows the variation in background intensity across a PBO AS fiber. A similar profile can be obtained for PBO HM. This was determined by the integration of a region in each diffraction pattern which did not include any distinct reflections. An idealized scattering curve is also plotted in Figure 5, calculated on the basis of a cylindrical, void-free fiber of uniform density, scaled to the experimental data.

Due to the low signal strength, the experimental data shown in Figure 5 are relatively noisy. However, this demonstrates that the features in Figure 4 are not evident in the across-fiber variations in diffuse-background scattering intensity. This therefore reduces the likelihood of density fluctuations or voids being responsible for the measured variations in layer line intensity. Furthermore, it validates the application of a model based upon a cylindrical fiber of uniform density. This particular result is in agreement with previous studies. For example, the skin of PBO AS is reported to be completely microvoid free,[14] while the heat treatment process is reported to cause microvoids to laterally collapse.[29]

The variations in molecular- and crystallographic-scale structural order which result in the changes in meridional layer line scattering arise due to a combination of factors. The most significant is probably domain orientation where, for the higher ordered layer lines, intensity contributions are only from highly axially oriented domains. Other factors may include crystallographic defects such as chain ends, impurities from processing, and conformational disorder. Lattice imaging techniques have previously reported axial disruptions in the PBO crystal lattice.[14] Equally, variations in chain packing could also affect the axial arrangement of molecules.[27,28,30,31] Thus, in this study the term "structural order", as measured from meridional scattering intensity, should be taken as representing a range of complimentary and competing morphological and crystallographic features.

Defining a PBO Fiber Model. By translating structural disorder to fiber morphology, the variations shown in Figure 4 can be employed to propose a model of skin−core fiber structure. This requires a suitable model definition based upon experimental observations (Figure 4), previous studies on PBO,[12,14] and other similar fiber types such as PPTA.[2−4,6−9] Most existing models suggest a dual-layer skin−core fiber structure.[4,5,7−9] This is in agreement with previous μ-XRD studies of PBO which report skin−core variations.[12] However, a recent study of PPTA suggests a three-layer model consisting of skin and core regions separated by an intermediate layer.[13] This structure is also supported by an AFM study which observed a small but distinct core in the locality of the center of the fiber.[3] The results observed in Figure 4 also suggest a three-layer structure. Both fibers exhibit a reduction in meridional scattering intensity corresponding to an inner core, with differences at the edges of the fibers indicating a skin structure. This combination of evidence provides a sound basis for the use of a three-layer morphological model in this current study.

The next model consideration is the nature of the transitional zones between different layers. A model proposed by Roth et al. utilizes explicit boundaries between different layers.[13] This was selected for modeling simplicity;[13] however, most experimental evidence suggests gradual transitions.[1,5,12] This is demonstrated with the gradual variation in crystalline domain orientation across the fiber axis.[1,5,12] Considering that many skin−core features occur as a consequence of environmental gradients during fiber processing, structural gradients should be somewhat expected. For example, this could be a temperature gradient during heat treatment or a shear-stress gradient during extrusion.[4] Consequently, a gradual transition between structural layers will be incorporated into the PBO fiber model.

The final consideration for this model is the definition of layer geometry. While most studies indicate a geometrically central core region, recent experimental evidence suggests that a geometrically offset core is also possible.[13] Considering the asymmetry shown in Figure 4, this feature will also be incorporated within this current model. However, the high degree of asymmetry in Figure 4 can only be satisfactorily explained by the core region being geometrically asymmetric. Thus, in this model, both the position and degree of asymmetry of the core region can be modified. A simplified diagram highlighting the model structure is shown in Figure 6. Note that the transitions between different layers are shown in Figure 6 explicitly for clarity (whereas the model utilizes gradual transitions).

This model assumes that the fiber exhibits short-range disorder while still maintaining long-range homogeneity. By definition, the model is a two-dimensional model of radial anisotropy. However, as μ-XRD is a transmission technique, the data shown in Figure 4 only provides one-dimensional information. No positional information is provided along the beam axis direction, only across the fiber axis. For certain model features such as the fiber skin, this limitation is inconsequential as the model inherently includes an assumption of fiber symmetry. However, the position of the core along the beam axis cannot be ascertained and is taken as being central. Furthermore, the core is assumed to be asym-

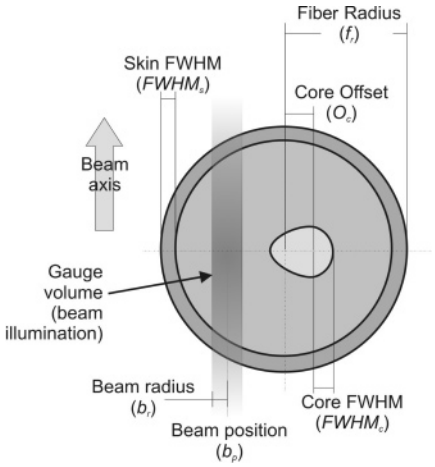

Figure 6. A schematic representation of the proposed PBO fiber model for structural disorder.

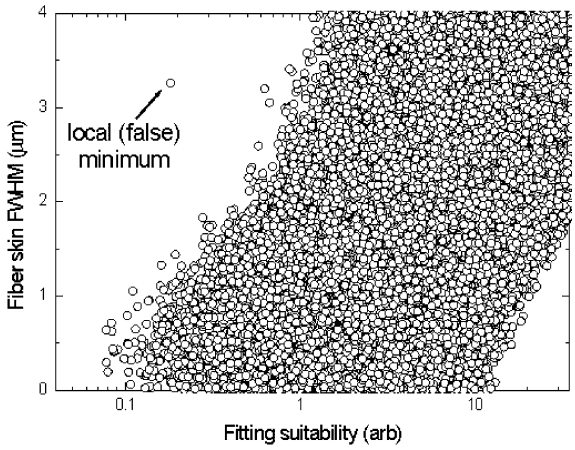

Figure 7. Correlation between fiber skin fwhm_s and fitting suitability. The plot shows a tendency toward (and evidence of) a single model minimum.

metric only on an axis perpendicular to the beam path (as this is the axis on which information is provided). Such assumptions are clearly a limitation to this modeling approach; however, this is consistent with previous μ-XRD studies.[13] Furthermore, the assumptions required for models based upon AFM, TEM, and SEM studies are perhaps more limiting as they require that microscopic, local observations are extrapolated to a macroscopic level.[3,4,6,9]

Model Implementation. Analytically, the model can be expressed in terms of a fiber diameter, defined within a matrix of 1^6 individual elements. For convenience, these can be thought of as consisting of collections of individual crystalline domains. The value held by each matrix element reflects the degree of structural order at that particular geometrical position within the model fiber. For simplicity, this value is restricted to a range between 0 and 1, reflecting total disorder and order, respectively. Thus, to define an idealized, homogeneous fiber with perfect internal organization, all elements hold values of unity. Calculation of the across-fiber scattering profile for such a fiber would yield the idealized profile shown in Figure 4.

For a radially anisotropic fiber, the degree of structural order for each element is assumed to be related to fiber morphology. Thus, it can be determined by the subtraction of disorder components reflecting the fiber skin and core from the ideal value (unity). For any given matrix coordinate (x, y), the degree of structural order ($I_{\text{total}(x,y)}$) can therefore be expressed in terms of the reduction from perfect order, due to the disordered skin and core components ($I_{s(x,y)}$ and $I_{c(x,y)}$):

$$I_{\text{total}(x,y)} = 1 - I_{s(x,y)} - I_{c(x,y)} \tag{1}$$

The requirement of a gradual transition between structural layers is provided by a Gaussian definition of disorder components. Thus, for an element at matrix coordinates (x, y), the disorder components relating to the fiber skin ($I_{s(x,y)}$) and core ($I_{c(x,y)}$) are given by

$$I_{c(x+O_C,y)} = \exp\left[-\left(\frac{x_r}{\text{fwhm}_c(1-A)}\right)^2\right]\exp\left[-\left(\frac{y_r}{\text{fwhm}_c}\right)^2\right] \tag{2}$$

$$I_{s(x,y)} = \exp\left[-\left(\frac{(x_r^{\,2}+y_r^{\,2})^{1/2}-f_r}{\text{fwhm}_s}\right)^2\right] \tag{3}$$

where x_r and y_r define the relative matrix positions from the fiber geometric center, the O_c parameter defines the positional offset of the core, and f_r is the fiber radius. The influence of both skin and core layers are dictated by the full width at half-maximum parameters (fwhm_s and fwhm_c). Additionally, the core component includes a core asymmetry parameter (A) whose sign varies in relation to the sign of the x_r parameter. Thus, variations in core asymmetry do not influence the fwhm_c value.

The meridional scattering intensity is assumed to be proportional to the degree of structural order. Thus, a model scattering intensity can be calculated by the addition of each element within an illuminated gauge volume (I_{bp}). This requires a model beam size and position to be defined proportionally to the model fiber diameter, on the basis of the ratio of the experimental beam to fiber dimensions. For a given beam radius (b_r) and position (b_p) the total scattering intensity is then given by

$$I_{bp} = \sum_{x=b_p-b_r}^{x=b_p+b_r}\sum_{y=1}^{y=1^6} I_{\text{total}(x,y)} \tag{4}$$

As only relative model intensities are required, the calculated scattering intensity series can be scaled for direct comparison with the experimental results. This is achieved using a least-squares fitting technique.

Monte Carlo Simulation. A Monte Carlo simulation was employed to determine optimum model parameters on the basis of the experimental results. The Monte Carlo method offers several advantages over other modeling techniques. By careful selection criteria it is possible to cover a large range of model permutations without favoring any particular solution. It is also possible to calculate fitting suitability as an arbitrary "goodness-of-fit" parameter given by summation of the absolute residuals. Cross-correlating fitting suitability against other model parameters ensures that there are no alternative parameter combinations which yield a similar solution. In this way, it is possible to verify whether any particular model solution is unique, or simply a single local minimum. This principle is shown in Figure 7 for 1.3^5 permutations where fiber skin fwhm_s is plotted against fitting suitability for PBO AS. It demonstrates how a model parameter converges as the fit to the experimental data improves (shown on a logarithmic scale for clarity). Figure 7 also highlights

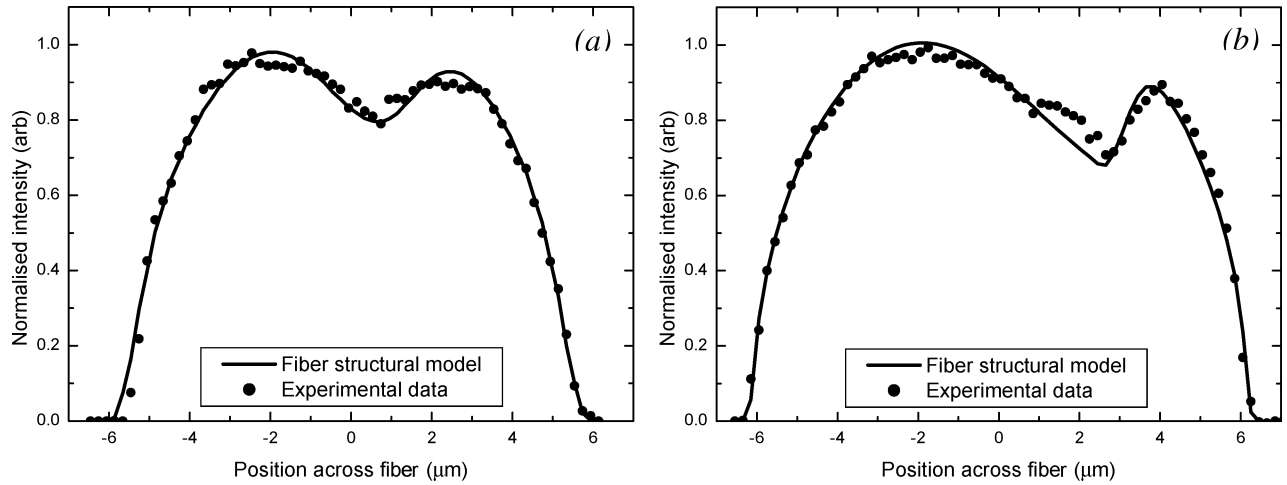

Figure 8. Across-fiber scattering intensities from the morphological models of PBO (a) AS and (b) HM compared against experimental results.

Table 1. Final Model Parameters for PBO AS and HM Disorder Models

	PBO AS	PBO HM		PBO AS	PBO HM
fiber radius (μm)	5.78 ± 0.11	6.20 ± 0.18	core offset (μm)	0.65 ± 0.15	2.50 ± 0.12
beam offset (μm)	0	0.1	core asymmetry (abs)	0.15 ± 0.11	0.65 ± 0.04
core fwhm (μm)	1.72 ± 0.06	2.32 ± 0.07	skin fwhm (μm)	0.40 ± 0.13	0.04 ± 0.18

how a specific local (false) minimum can be excluded as the real solution. Finally, the Monte Carlo method enables an estimation of model error to be calculated, on the basis of the correlation between model parameter variations and fitting suitability.

For this study two Monte Carlo simulations were used in series for each fiber model, comprising two sets of 2.5^5 individual permutations. For both simulations the parameters were initially described by a normal distribution to avoid artificially favoring any given solution. The first simulation was performed using a large distribution to maximize the range of model structures assessed. The resulting "optimized" parameters were then reused as the basis for a second confined simulation, within a more limited distribution range. This series-simulation approach provides a means of finding an approximate global minimum and then refining the model to provide the best overall local fit.

Results

Figure 8 shows the across-fiber scattering intensity profiles from the morphological models of PBO AS and HM. Also plotted in Figure 8 are the experimental values for direct comparison. In both cases the model provides a good fit to the results obtained experimentally. This validates the translation of structural order into a three-layer skin−core morphological model. The only feature which is not accounted for in the model is the region of increased intensity around 2 μm for PBO HM. This occurs close to, but not coincidentally with, the local intensity minimum at about 2.5 μm, presumed to indicate the center of the morphological core. This feature suggests a further level of complexity to the core region which has yet to be explained by the current model.

A second model was also tried utilizing an explicit boundary between the different structural layers, as used in a previous study.[13] This second model was unable to fit the experimental data in a satisfactory manner. Consequently, the use of gradual transition zones between layers in this model is further validated. The final model parameters which provide the best fit to the experimental data for both fiber types are collected in Table 1.

While the results in Table 1 indicate the differences between the two model solutions, it is perhaps more useful to visualize the models directly. In this case, such a visualization is relatively straightforward as the structural order value for each model element can be converted to intensity. The visualizations are shown in Figure 9, with each element shown with an intensity component denoting the scattering contribution (the level of order). The black regions specify disordered areas.

Discussion

The three-layer model proposed by this study provides a good correlation with the experimental results obtained for both fiber types (Figure 8). Variations between the individual model parameters can therefore be used to make comparisons. This permits the investigation of morphological changes occurring through the heat treatment process. If the fiber radius results shown in Table 1 are first compared, the AS fiber exhibits a much smaller fiber radius than PBO HM. This is also evident from Figure 4 directly. This difference is the inverse of previous SEM-based studies which suggest heat treatment to reduce the fiber diameter.[19] One explanation for this might be the diameter variations resulting from the coagulation process.[19,29] Previous SEM studies have reported standard deviations of up to 1 μm.[19] To demonstrate this, Figure 10 shows SEM measurements of PBO AS and HM fiber diameters. The fibers selected in the images exhibit the same diameters as the model values obtained for each fiber type. The ease with which it is possible to obtain such correlations demonstrates that large diameter variations are commonplace. Alternatively, the PBO AS fiber diameter could be underestimated from X-ray diffraction-based experiments if there were an amorphous skin layer around the fiber. This latter hypothesis is supported by the larger skin fwhm parameter for the as-spun fiber

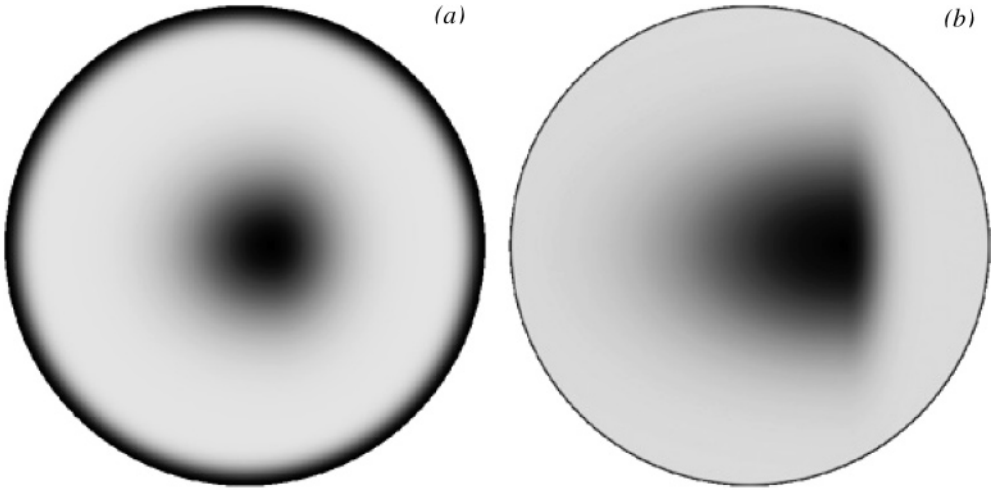

Figure 9. Visualizations of structural disorder models for PBO (a) AS and (b) HM. The level of disorder is scaled from light gray (ordered) to black (disordered).

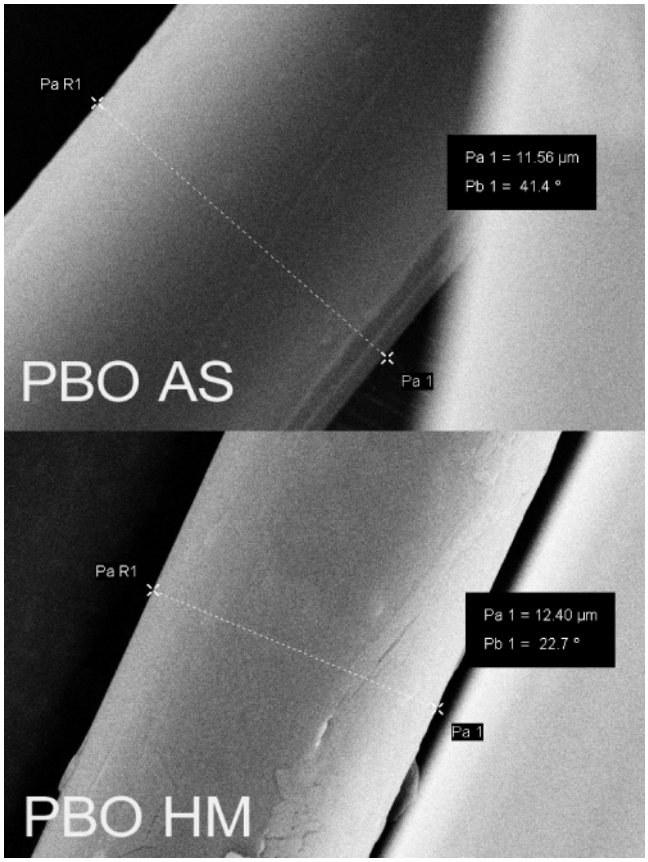

Figure 10. SEM measurements of PBO AS and HM fiber diameter. Fibers are shown which exhibit the same diameter as those obtained through the model results.

type in comparison with PBO HM. Furthermore, a purely amorphous skin layer of up to 1 μm thickness was previously proposed for the PPTA fiber type.[2] This explanation still cannot explain the differences observed in the diameter of the PBO HM fiber between this and previous studies.[19]

The fact that the as-spun fiber exhibits a relatively disordered skin layer is itself interesting. Studies of the PPTA fiber type report the skin region to consist of well-packed and uniform fibrils.[6] This morphology is thought to be shared by PBO fibers which exhibit a skin region without voids.[14] Therefore, while the skin appears more organized on a fibrillar level, it is clearly less organized on molecular and crystallographic scales. The modeling results also indicate that there are significant differences in skin thickness (fwhm) between PBO fiber types. While a thick skin is favored for PBO AS, the skin of the heat-treated fiber is approximately 10 times thinner. Thus, heat treatment directly reduces structural disorder within the fiber skin region. Previous studies on PBO have reported transverse crystallite growth between the edges of heterocyclic rings during heat treatment.[28,32] Therefore, the HM fiber undergoes a general improvement in crystallinity and a reduction in paracrystalline disorder.[14,28,29,32] Furthermore, the heat-treated fiber is reported to have a higher degree of crystalline domain orientation than the as-spun fiber, within both skin and core regions.[12] Such changes are consistent with the results suggested by the structural disorder model.

While these changes in the skin during heat treatment seem relatively straightforward, the PBO fiber core results are less clear. Both fiber types exhibit a significant core region with a reduction in structural order indicated by a reduced meridional layer line intensity. Kitagawa et al. also report less meridional intensity in the core region of the PBO AS fiber type from electron diffraction.[14] However, the core size (fwhm) is smaller in the as-spun fiber compared to the HM fiber type. Considering the aforementioned reduction in skin disorder during heat treatment, this result remains as yet unexplained. A modeling error can almost certainly be ruled out, as the core difference can also be observed directly from the experimental results shown in Figure 4.

One of the most significant differences between the core regions of the two PBO fiber types is the variation in core position and asymmetry. In the AS fiber, the symmetrical core is positioned coincidentally with the geometric center of the fiber. By contrast, the HM fiber exhibits a core which is highly asymmetric and positioned away from the geometric fiber center. Thus, the heat treatment process influences the morphology of the fiber core region, as reported in previous studies for PPTA.[13] Such changes must occur due to the imposition of unequal mechanical forces and/or heating during the heat treatment process. This could be explained by a number of common processing procedures. Winding the heat-treated fiber onto a bobbin while still at high temperature would be one explanation, as would per-

forming heat treatment by drawing the fiber over a heated surface. With detailed information regarding the manufacture of the PBO fiber type being proprietary, a precise explanation cannot be given. However, such a feature of these fiber types may directly impact experimental results obtained using highly localized probing techniques. For example, samples representing fiber core regions are often collected from the fiber geometrical center, which may not necessarily coincide with the morphological center.

Conclusions

Diffraction patterns can be successfully obtained from single fibers using one-dimensional waveguide optics. This allows skin−core structure to be studied with minimal averaging across the fiber width. Furthermore, unlike other techniques, X-ray diffraction can be performed in transmission without the need for sample modification. In this particular case, variations in across-fiber meridional scattering intensity can be related to the degree of structural order. Through the association of disorder with morphological layers, a fiber model has been proposed. This describes the structure of PBO using a three-layer model consisting of skin, core, and intermediate regions, between which are gradual transitions. By the application of a Monte Carlo simulation, a good correlation is achieved between the model and experimental data.

Heat treatment of PBO causes a number of significant structural changes to occur in fiber morphology. For example, there is a significant reduction in the size of the fiber skin region, while the position of the fiber core shifts. Consequently, the HM fiber type exhibits a core that is no longer coincidental with the geometric center of the fiber and is also highly asymmetric. How this structural asymmetry influences other testing techniques is unknown. It will certainly be of critical importance when selecting regions of fiber to study using highly localized probing techniques. The variations in the fiber skin region are also important for spectroscopic methods applied to single fibers. For example, results collected with Raman spectroscopy should be sensitive to such variations due to the limited laser light penetration depths for most opaque polymers.[1]

The experiment has also highlighted several important differences which cannot be currently explained. These include the intensity feature in the PBO HM profile shown in Figure 4 and the larger core fwhm in PBO HM. These serve to highlight areas where gaps exist in the present understanding of fiber skin−core morphology. How the skin−core variations must impact upon mechanical properties is also unclear. For example, some previous studies have suggested that skin−core morphology may enhance tensile properties by terminating cracks.[2] Alternatively, other studies propose that any skin−core difference may encourage areas of stress concentration.[30]

Acknowledgment. We thank Toyobo (Japan) for the supply of PBO fiber samples used in this study. The waveguide was developed at the Budker Institute of Nuclear Physics (Novosibirsk, Russia) within the context of a collaboration with Sincrotrone Trieste. A. Snigirev is acknowledged for the PBO fiber SEM images.

References and Notes

(1) Young, R. J.; Lu, D.; Day, R. J.; Knoff, W. F.; Harris, H. A. *J. Mater. Sci.* **1992**, *27*, 5431−5440.
(2) Graham, J. F.; McCague, C.; Warren, O. L.; Norton, P. R. *Polym. Commun.* **2000**, *41*, 4761−4764.
(3) Li, S. F. Y.; McGhie, A. J.; Tang, S. L. *Polymer* **1993**, *34*, 4573−4575.
(4) Morgan, R. J.; Pruneda, C. O.; Steele W. J. *J. Polymer Sci., Polym. Phys. Ed.* **1983**, *21*, 1757−1783.
(5) Riekel, C.; Dieing, T.; Engstrom, P.; Vincze, L.; Martin, C.; Mahendrasingam, A. *Macromolecules* **1999**, *32*, 7859−7865.
(6) Panar, M.; Avakian, P.; Blume, R. C.; Gardner, K. H.; Gierke, T. D.; Yang, H. H. *J. Polymer Sci., Polym. Phys. Ed.* **1983**, *21*, 1955−1969.
(7) Rebouillat, S.; Peng, J. C. M.; Donnet, J. B. *Polymer* **1999**, *40*, 7341−7350.
(8) Vezie, D. L.; Thomas, E. L.; Adams, W. W. *Polymer* **1995**, *36*, 1761−1779.
(9) Li, L. S.; Allard, L. F.; Bigelow, W. C. *J. Macromol. Sci., Phys.* **1983**, *B22*, 269−290.
(10) Muller, M.; Riekel, C.; Vuong, R.; Chanzy, H. *Polymer* **2000**, *41*, 2627−2632.
(11) Riekel, C. *Rep. Prog. Phys.* **2000**, *63*, 233−262.
(12) Davies, R. J.; Montes-Moran, M. A.; Riekel, C.; Young, R. J. *J. Mater. Sci.* **2003**, *38*, 2105−2115.
(13) Roth, S.; Burghammer, M.; Janotta, A.; Riekel C. *Macromolecules* **2003**, *36*, 1585−1593.
(14) Kitagawa, T.; Murase, H.; Yabuki, K. *J. Polym. Sci., Part B: Polym. Phys.* **1998**, *36*, 39−48.
(15) Kitagawa, T.; Yabuki, K.; Young, R. J. *Polymer* **2001**, *42*, 2101−2112.
(16) Choe, E. W.; Kim, S. N. *Macromolecules* **1981**, *14*, 920−924.
(17) Kumar, S. In *Enyclopedia of composites*; Lee, S. M., Ed.; VCH Publishing: New York, 1990; Vol. 14, p 51.
(18) Wolfe, J. F. In *Encyclopedia of Polymer Science and Engineering*, Mark, H. F., Ed.; John Wiley and Sons: New York, 1988; Vol. 11, p 601.
(19) Davies, R. J.; Montes-Moran, M. A.; Riekel, C.; Young, R. J. *J. Mater. Sci.* **2001**, *36*, 3079−3087.
(20) Jark, W.; DiFonzo, S.; Lagomarsino, S.; Cedola, A.; diFabrizio, E.; Bram, A.; Riekel, C. *J. Appl. Phys.* **1996**, *80*, 4831−4836.
(21) Hammersley A. P.; Svensson S. O.; Thompson A. *Nucl. Instrum. Methods Phys.* **1994**, *346*, 312−321.
(22) Hammersley, A. P.; Svensson, S. O.; Thompson, A.; Graafsma, H.; Kvick, Å.; Moy, J. P. *Rev. Sci. Instrum.* **1995**, *66*, 2729−2733.
(23) Fratini, A. V.; Lenhert, P. G.; Resch, T. J.; Adams, W. W. *Mater. Res. Symp. Proc.* **1989**, *134,* 431.
(24) Young, R. J.; Day, R. J.; Zakikhani, M. *J. Mater. Sci.* **1990**, *25*, 127−136.
(25) So, C. L.; Young, R. J. *Plast. Rubber Compos. Process. Appl.* **1997**, *26*, 423.
(26) Kumar, S.; Warner, S.; Grubb, D. T.; Adams, W. W. *Polymer* **1994**, *35*, 5408−5412.
(27) Martin, D. C.; Thomas, E. L. *Mater. Res. Symp. Proc.* **1989**, *134*, 415.
(28) Martin, D. C.; Thomas, E. L. *Macromolecules* **1991**, *24*, 2450−2460.
(29) Hunsaker, M. E.; Price, G. E.; Bai, S. J. *Polymer* **1992**, *33*, 2128−2135.
(30) Kitagawa, T. In *Encyclopedia of Materials: Science and Technology*; Buschow, K. H. J., Cahn, R. W., Flemings, M. C., Ilschner, B., Kramer, E. J., Mahajan S., Eds.; Elsevier Science: New York, 2001; pp 7276−7280.
(31) Tashiro, K.; Yoshino, J.; Kitagawa, T.; Murase, H.; Yabuki, K. *Macromolecules* **1998**, *31*, 5430−5440.
(32) Krause, S. J.; Haddock, T. B.; Vezie, D. L.; Lenhert, P. G.; Hwang, W.-F.; Price, G. E.; Helminiak, T. E.; O'Brien, J. F.; Adams, W. W. *Polymer* **1988**, *29*, 1354−1364.

MA048209A